Analysis of Heartbeat Dynamics by Point Process Adaptive Filtering

Riccardo Barbieri*, *Member, IEEE,* and Emery N. Brown, *Member, IEEE*

***Abstract*—Heartbeats are a point process yet, most of the current analysis methods do not model this important characteristic of these data. We describe human heartbeat time series as a history dependent inverse Gaussian model. We present a point process adaptive filter algorithm to estimate the model's time-varying parameters, and use it to compute new measures of heart rate variability. We apply our algorithm to analyze simulated heartbeat data and actual heartbeat data from a tilt table experiment and from healthy subjects and subjects with congestive heart failure during sleep. Our results suggest a new approach for characterizing heartbeat dynamics.**

***Index Terms*—Adaptive filters, heart rate variability, point processes, state estimation.**

I. Introduction

HEART rate and heart rate variability (HRV) are important dynamic measures of the state of the cardiovascular system and the autonomic nervous system. Heart rate is traditionally estimated as the average of the reciprocal of the R–R intervals within a specified time window, or as the number of R-wave events (heartbeats) per unit time on the electrocardiogram (ECG). The current approaches to characterizing HRV include elementary statistical measures of the properties of the R–R intervals [1], spectral analysis of heart rate or R–R interval time-series [1]–[8], deterministic dynamical systems assessments of heart rate signal properties [9]–[12], and approximate entropy measures of R–R interval regularity [13].

Several issues in these approaches to deriving heart rate and HRV from R-wave events have yet to be addressed. First, the R-wave events mark the electrical impulses from the heart's conduction system that represent ventricular contractions. Hence, they are a sequence of discrete occurrences in continuous time, and as such, form a point process. Rather than modeling them to reflect the point process structure of the heartbeats, current methods either treat the heartbeat series or R–R interval as continuous-valued signals, or convert R–R interval data into continuous-valued, evenly spaced measurements for analysis by interpolation of either the R–R intervals or their reciprocals. Second, in addition to some form of interpolation, application of the frequency domain methods requires the ECG to be recorded under stationary conditions. Nonstationary analysis approaches apply time-varying methods to R–R interval [14]–[17] or to heart rate [5], [18] time series obtained by interpolation of the R–R intervals or the reciprocal of the R–R interval beat series, respectively. In contrast, current methods that do not interpolate do not have a temporal resolution smaller than two consecutive R–R intervals [6], [19]–[21]. Furthermore, current methods do not characterize the stochastic structure of the heartbeats beyond giving a single mean and variability index of either R–R intervals or heart rate series. Finally, adaptive filter algorithms for point processes have been recently designed to characterize the dynamic properties of neural systems such as the representation of biological signals in ensemble spiking activity and plasticity in neural receptive fields [22]–[24]. Despite the point process structure of the heartbeats, and their dynamic control by the autonomic nervous systems, point process adaptive filter algorithms have not been used to analyze heartbeat dynamics.

To address these issues, we use the recently developed history-dependent inverse Gaussian (HDIG) point process model of heartbeat intervals to study the problem of characterizing heartbeat interval dynamics [25]. This model gives precise probabilistic definitions of heart rate and HRV that can be updated at any desired time resolution. We estimate the time-varying parameters of the HDIG point process model by point process adaptive filtering, and assess model goodness-of-fit by a Kolmogorov–Smirnov (KS) test derived from the time-rescaling theorem [26]. We illustrate the point process adaptive filtering approach to characterizing heartbeat dynamics in a study of simulated heartbeat interval series under stationary and nonstationary conditions, in the analysis of the heartbeat interval series from a subject in a tilt table study, and in a comparison of HRV between healthy subjects and subjects with congestive heart failure.

II. Methods

In this section, we present the heartbeat interval and the heart rate probability models, the state-space model for the heartbeat interval model parameters, the point process adaptive filtering algorithm to derive instantaneous estimates of heart rate and HRV, and goodness-of-fit tests to evaluate how well these estimates describe the stochastic structure of a time-series of heartbeats, or R-wave events extracted from an ECG. We begin the

Manuscript received October 1, 2004; revised March 6, 2005. This work was supported in part by the National Institutes of Health (NIH) under Grant MH59733, Grant MH61637, Grant MH65018, and Grant DA015644, in part by the National Science Foundation (NSF) under Grant 0081548, and in part by grants from the Defense Advanced Research Projects Agency (DARPA) and the Office of Naval Research (ONR). *Asterisk indicates corresponding author.*

*R. Barbieri is with the Neuroscience Statistics Research Laboratory, Department of Anesthesia and Critical Care, Massachusetts General Hospital, Boston, MA 02114-2696 USA (e-mail: barbieri@neurostat.mgh.harvard.edu).

E. N. Brown is with the Neuroscience Statistics Research Laboratory, Department of Anesthesia and Critical Care, Massachusetts General Hospital, Boston, MA 02114 USA and the Department of Brain and Cognitive Sciences, MIT/Harvard Medical School Division of Health Sciences and Technology, Massachusetts Institute of Technology, Cambridge, MA 02139 USA. (e-mail: brown@neurostat.mgh.harvard.edu).

Digital Object Identifier 10.1109/TBME.2005.859779

derivation of our heartbeat probability model by reviewing the physiology of the R-wave events.

A. Physiology of the Heartbeat

Each R-wave event is initiated by a coordinated depolarization of the heart's pacemaker cells that begins in the sino-atrial (SA) node of the right atrium and then propagates through its specialized conduction system to the left atrium and to the two ventricles [27]. Like a nerve cell action potential, each depolarization is accomplished by an exchange of sodium, potassium and calcium ions across the pacemaker cell membrane causing a rise in the cell's transmembrane potential. Once the membrane reaches the cell's threshold, depolarization occurs. Following each depolarization, the transmembrane potentials of these cells return to their resting potentials and they begin again their spontaneous rise toward threshold [27]. When there is normal coupling of electrical and mechanical events in the heart, the R-wave on the ECG is used as a standard marker of ventricular contraction or the time of a heartbeat. Deterministic models of this integrate (rise of the transmembrane potential)-and-fire (depolarization) mechanism are used regularly to simulate heartbeats or R-wave events [28], [29]. An elementary, stochastic integrate-and-fire model is the Gaussian random walk model with drift. The probability density of the first passage times for this random walk process, i.e., the times between threshold crossings (R–R intervals), is well-known to be the inverse Gaussian [30]. Under this model, the R–R intervals are independent and thus, form a renewal process [30]. Because the inverse Gaussian probability density is derived directly from an elementary, physiologically-based integrate-and-fire model, it has been used to study neural processes [30] and heartbeats [31].

Although the inverse Gaussian model is a good starting point for developing a statistical model of heartbeats, the physiology of the heartbeat mechanism suggests two further modifications. First, because the parasympathetic and sympathetic inputs to the SA node can occur on a millisecond time-scale but their effects can last for several seconds, the R–R intervals must be modeled as dependent on the recent history of the SA node inputs and not as independent. Second, sympathetic and parasympathetic inputs to the SA node are an important dynamic part of the cardiovascular control circuitry. Thus, these autonomic inputs are continuously altering the propensity of the SA node to initiate heartbeats to maintain homeostasis. Therefore, in considering the effect of the recent history of autonomic inputs to the SA node, a heartbeat probability model must take into account the dynamic or time-varying nature of these inputs.

B. A Probability Model of Heartbeat Intervals

We assume that in an observation interval $(0, T]$, we record $0 < u_1 < u_2 <, \ldots, < u_k <, \ldots, < u_K \leq T$, K successive R-wave event times from an ECG. We assume that given any R-wave event u_k, the waiting time until the next R-wave event, or equivalently, the length of the next R–R interval, obeys a HDIG probability density $f(t|H_k, \theta)$, where t is any time satisfying $t > u_k$, H_k is the history of the R–R intervals up to u_k, and θ is a vector of model parameters [25], [31]. The model is defined as

$$f(t|H_k,\theta) = \left[\frac{\theta_{p+1}}{2\pi(t-u_k)^3}\right]^{\frac{1}{2}} \times \exp\left\{-\frac{1}{2}\frac{\theta_{p+1}\left[t-u_k-\mu(H_k,\theta)\right]^2}{\mu(H_k,\theta)^2(t-u_k)}\right\} \quad (1)$$

where $H_k = \{u_k, w_k, w_{k-1}, \ldots, w_{k-p+1}\}$, $w_k = u_k - u_{k-1}$ is the kth R–R interval, $\mu(H_k,\theta) = \theta_0 + \sum_{j=1}^{p}\theta_j w_{k-j+1} > 0$ is the mean, $\theta_{p+1} > 0$ is the scale parameter, and $\theta = (\theta_0, \theta_1, \ldots, \theta_{p+1})$. This model represents the dependence of the R–R interval length on the recent history of parasympathetic and sympathetic inputs to the SA node by modeling the mean as a linear function of the last p R–R intervals. If we take $p = 0$, the R–R intervals are independent, then $\mu(H_k,\theta) = \theta_0$, $f(t|H_k,\theta) = f(t|u_k,\theta_0,\theta_1)$, and (1) becomes a simple renewal inverse Gaussian model.

The mean and standard deviation of the R–R probability model in (1) are, respectively

$$\mu_{\mathrm{RR}} = \mu(H_k,\theta) \quad (2)$$

$$\sigma_{\mathrm{RR}} = \left[\mu(H_k,\theta)^3\theta_{p+1}^{-1}\right]^{\frac{1}{2}}. \quad (3)$$

From (2) and (3) it follows that both μ_{RR} and σ_{RR} are time-dependent. We use the probability density in (1) to define heart rate and HRV. Heart rate is often defined as the reciprocal of the R–R intervals [5], [8], [18], [32]–[35]. For any $t > u_k$, $t - u_k$ is the waiting time until the next R-wave event. We define $r = c(t-u_k)^{-1}$ as the heart rate random variable, where $c = 6 \times 10^4$ ms/min is the constant that converts the R–R interval measurements recorded in milliseconds into heart rate measurements in beats per minute (bpm). Therefore, because r is a one-to-one transformation of $t - u_k$, we use the standard change-of-variables formula from elementary probability theory [26] and derive from the R–R interval probability density in (1), the heart rate probability density $f(r|H_k,\theta)$ defined as

$$f(r|H_k,\theta) = \left|\frac{dt}{dr}\right| f(t|H_k,\theta) = \left[\frac{\theta^*_{p+1}}{2\pi r}\right]^{\frac{1}{2}} \exp\left\{-\frac{1}{2}\frac{\theta^*_{p+1}\left[1-\mu^*(H_k,\theta)r\right]^2}{\mu^*(H_k,\theta)^2 r}\right\} \quad (4)$$

where $\mu^*(H_k,\theta) = c^{-1}\mu(H_k,\theta)$ and $\theta^*_{p+1} = c^{-1}\theta_{p+1}$. The mean and standard deviation of the heart rate probability density are, respectively

$$\mu_{\mathrm{HR}} = \mu^*(H_k,\theta)^{-1} + {\theta^*_{p+1}}^{-1} \quad (5)$$

$$\sigma_{\mathrm{HR}} = \left[\frac{2\mu^*(H_k,\theta)+\theta^*_{p+1}}{\mu^*(H_k,\theta)\cdot{\theta^*_{p+1}}^2}\right]^{\frac{1}{2}}. \quad (6)$$

Equation (4) defines the stochastic properties of heart rate in terms of a probability density. If $p = 0$, then (4) gives the simple reciprocal of the inverse Gaussian probability density discussed

in [36]. Because the mean is a representative value of the probability density we define heart rate as the mean (5) of $f(r|H_k,\theta)$, and the heart rate variance as the square of the standard deviation (6).

The probability density (1) for the R–R intervals, $f(t|H_k,\theta)$, models the effect of recent sympathetic and parasympathetic input to the SA node through the history dependence in its mean parameter, $\mu(H_k,\theta)$. Unlike in the Gaussian probability density, the standard deviation of the inverse Gaussian distribution is a function of the mean (3). The R–R interval probability model is transformed into the heart rate probability density, $f(r|H_k,\theta)$ (4) through a standard change-of-variable relation. The mean (5) and the standard deviation (6) of the heart rate probability model, like those of the heartbeat probability model, are history-dependent and the standard deviation is a function of the mean.

C. A Point Process Adaptive Filter Algorithm

To track the nonstationary behavior in heartbeat dynamics that occurs due to changes in state under both physiological and pathological conditions, we assume that the parameter θ is time-varying, and we model the time-varying behavior of θ using a state space model. To define the state model and the observation model, we choose J large, and divide $(0,T]$ into J intervals of equal width $\Delta = T/J$, so that there is at most one spike per interval. The adaptive parameter estimates will be updated at $j\Delta$ for $j = 1,\ldots,J$. We assume that the temporal dynamics of the parameter θ are described by the following random walk state model:

$$\theta_j = \theta_{j-1} + \varepsilon_j \tag{7}$$

where ε_j is a Gaussian noise with zero mean and covariance matrix W_ε.

From the heartbeat probability model in (1) we define the associated conditional intensity function as

$$\lambda(j\Delta|H_j,\theta_{j\Delta}) = \frac{f(j\Delta|H_j,\theta_{j\Delta})}{1-\int_{u_j}^{j\Delta} f(u|H_j,\theta_u)du}. \tag{8}$$

The conditional intensity function provides a canonical characterization of a point process that gives a history-dependent generalization of the rate function of a Poisson process [37]. For a small interval Δ, $\lambda(j\Delta|H_j,\theta_{j\Delta})\Delta$ defines the probability of an event in the interval $((j-1)\Delta, j\Delta]$. Let n_j be 1 if a heartbeat occurs in $((j-1)\Delta, j\Delta]$ and 0 otherwise. To complete our state space representation of the heartbeat process we use the representation of the probability mass function in terms of the conditional intensity function to define our observation model [37]. For Δ small, the probability mass function for the occurrence of an R-wave event in the interval $((j-1)\Delta, j\Delta]$ may be written as [23], [24], [37]

$$\Pr(n_j|H_j,\theta_j) = \exp\{n_j \log[\lambda(j\Delta|H_j,\theta_{j\Delta})\Delta] - \lambda(j\Delta|H_j,\theta_{j\Delta})\Delta\}. \tag{9}$$

Given the state model in (7) and the observation process model in (9), it follows from [23], [24] that the point process adaptive filter algorithm for this system is

(*One-Step Prediction*)

$$\theta_{j|j-1} = \theta_{j-1|j-1} \tag{10}$$

(*One-Step Prediction Variance*)

$$W_{j|j-1} = W_{j-1|j-1} + W_\varepsilon \tag{11}$$

(*Posterior Mode*)

$$\theta_{j|j} = \theta_{j|j-1} + W_{j|j-1}(\nabla \log \lambda_j)[n_j - \lambda_j\Delta] \tag{12}$$

(*Posterior Variance*)

$$W_{j|j} = \left[W_{j|j-1}^{-1} - (\nabla^2 \log \lambda_j)[n_j - \lambda_j\Delta] - (\nabla \log \lambda_j)[\nabla\lambda_j\Delta]'\right]^{-1} \tag{13}$$

where $\lambda_j = \lambda(j\Delta|H_j,\theta_{j|j-1})$ and $\nabla(\nabla^2)$ denotes the first (second) derivative of the indicated function with respect to θ for $j = 1,\ldots,J$. The notation $\theta_{j|k}$ defines the state at time $j\Delta$ given the observations from $(0,k\Delta]$.

Equations (10)–(13) provide a recursive Gaussian approximation for estimating the hidden state process (7), observed through a point process (9), the same way the well-known Kalman filter provides a way of estimating a linear Gaussian state process observed through Gaussian measurements [38]. Here, the point process is the heartbeats and the hidden state is the assumed time-varying parameter θ_j of the heartbeat model. The logic of the algorithm is as follows. Given at time $(j-1)\Delta$ the state estimate $\theta_{j-1|j-1}$ and its variance estimate $W_{j-1|j-1}$ based on the heartbeat observations in $(0,(j-1)\Delta]$, the algorithm first predicts $\theta_{j|j-1}$, the estimate of the state at time $j\Delta$ (10), and $W_{j|j-1}$, the uncertainty in the state estimate at time $j\Delta$, given the heartbeat observations in $(0,(j-1)\Delta]$ (11). Once the measurement at time $j\Delta$ is observed, $\theta_{j|j}$, the state estimate at time $j\Delta$ is computed as a combination between the one-step prediction estimate $\theta_{j|j-1}$ and a correction term which is determined by the observation. The correction term has two components: a weight determined by the one-step prediction variance $W_{j|j-1}$ and $\nabla \log \lambda_j$, and the point process innovation term $[n_j - \lambda_j\Delta]$. The innovation defines how the heartbeat data enter the algorithm by computing the difference between $\lambda_j\Delta$, the probability of a heartbeat at time $j\Delta$ and n_j whether or not a heartbeat occurs at time $j\Delta$. To complete computation at time $j\Delta$, the algorithm also estimates $W_{j|j}$, the uncertainty in the state at time $j\Delta$ given the data in $(0,j\Delta]$. The algorithm is nonlinear because $\theta_{j|j}$ appears on the left-hand and right-hand side of (12) because λ_j is a function of $\theta_{j|j}$. Therefore, these equations must be solved at each time $j\Delta$ by Newton's method using $\theta_{j|j-1}$ as a starting estimate.

Given $\theta_{j|j}$, the point process adaptive filter estimate of θ at time $j\Delta$, it follows from (2), (3), (5), and (6), that the instantaneous estimates of mean R–R, R–R interval standard deviation, mean heart rate and heart rate standard deviation at time $j\Delta$ are, respectively

(*Mean R–R Interval*)

$$\mu_{RR}(j\Delta) = \mu(H_j,\theta_{j|j}) \tag{14}$$

(*R–R Interval SD*)

$$\sigma_{\mathrm{RR}}(j\Delta) = \left[\mu(H_j,\theta_{j|j})^3\theta^{-1}_{p+1,j|j}\right]^{\frac{1}{2}} \tag{15}$$

(*Mean Heart Rate*)

$$\mu_{\mathrm{HR}}(j\Delta) = \mu^*(H_j,\theta_{j|j})^{-1} + \theta^*_{p+1,j|j}{}^{-1} \tag{16}$$

(*Heart Rate SD*)

$$\sigma_{\mathrm{HR}}(j\Delta) = \left[\frac{2\mu^*(H_j,\theta_{j|j}) + \theta^*_{p+1,j|j}}{\mu^*(H_j,\theta_{j|j})\cdot\theta^*_{p+1,j|j}{}^2}\right]^{\frac{1}{2}}. \tag{17}$$

Equation (16) provides a new algorithm for computing an instantaneous estimate of heart rate whereas (15) and (17) are new indices of HRV.

D. Model Goodness-of-Fit

To evaluate goodness-of-fit for the heartbeat probability model-point process adaptive filter algorithm, i.e., determine how well this model describes the sequence of ECG R-wave events, we use the KS test based on the time-rescaling theorem for point processes [26]. The method uses the estimated conditional intensity function to construct a transformation of the $R{-}R$ intervals that maps them to independent observations on the interval (0,1]. Agreement between the transformed observations and the uniform probability density can be assessed by the KS test and the estimated autocorrelation function is used to assess whether the temporal structure in the transformed observations is consistent with the transformed intervals being independent. Because the time-rescaling transformation is one-to-one, close agreement between the transformed $R{-}R$ intervals and the uniform probability density implies close agreement between the original $R{-}R$ intervals and the particular model from which the conditional intensity function was estimated.

III. Results

A. Analysis of a Simulated Heartbeat Series Under Constant Conditions

Many studies of heartbeat interval dynamics are conducted under constant conditions. Therefore, we first tested the ability of our point process adaptive filter algorithm to estimate simulated heartbeat interval data from the HDIG heartbeat probability model (1) in which the parameter θ was constant. Because of the definition of the HDIG mean, these simulated data were still highly correlated as the expected length of the $R{-}R$ interval depended on the p previous intervals. However, the coefficients describing that relation were constant in time. Using the Gaussian approximation to the inverse Gaussian probability density [38], we simulated 1600 s (26.67 min) of heartbeat series using the history dependent inverse Gaussian model of order $p = 2$ and parameters $\theta_0 = 834$ ms, $\theta_1 = -0.15$, $\theta_2 = -0.25$, and $\sigma^2_{\mathrm{RR}} = 750$ ms^2. By (6) the parameter θ_3 was chosen implicitly by defining θ_0, θ_1, θ_2, and σ^2_{RR}. These

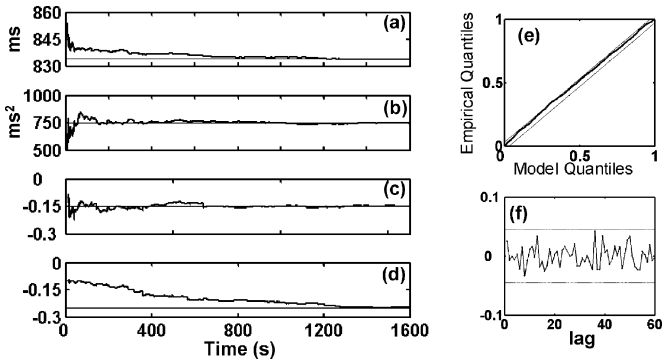

Fig. 1. Estimates from a stationary AR(2) simulated beat series of (a) the θ_0 parameter, (b) the variance σ^2_{RR}, and (c) and (d) the autoregressive parameters θ_1 and θ_2. The one-step prediction variance (11) is set as equal to the posterior variance computed at the previous step (13). (e) KS plots of the time-rescaled quantiles derived from the parameters' estimates. The proposed model is considered consistent with the data if its KS plot falls within the 95% confidence bounds, defined by the parallel black lines in the panel. (f) Autocorrelation function of the transformed times for the first 60 lags. The horizontal lines are the approximate 95% confidence intervals.

parameter values gave an average heart rate of 50 bpm. For this application of the point process adaptive filter algorithm, we chose the deterministic state space model with $W_\varepsilon = 0$ and an update interval $\Delta = 5$ ms. We tested the algorithm by picking initial guesses of the parameters as random numbers drawn from the uniform probability density $\theta_i \pm 0.5\theta_i$ for $i = 0,\ldots,2$ and a random number from the uniform probability density $\sigma^2_{\mathrm{RR}} \pm 0.5\sigma^2_{\mathrm{RR}}$.

Fig. 1 illustrates an application of the point process adaptive filter algorithm with starting values $\theta_0 = 855$ ms, $\theta_1 = \theta_2 = -0.1$, and $\sigma^2_{\mathrm{RR}} = 500$ ms^2. Following a rapid decline in the first 50 s toward the true value of θ_0, the estimate of θ_0 slowly approached the true value and did not converge to it until 775 s [Fig. 1(a)]. Within less than 100 s the estimates of σ^2_{RR} began to estimate the true parameter value [Fig. 1(b)] and similarly, the estimates of θ_1 approached the true value almost immediately [Fig. 1(c)]. The estimate of θ_2 declined linearly and did not converge to the true value until 1200 s [Fig. 1(d)]. The convergence of the point process adaptive filter estimates to the true parameter values in this example is analogous to the convergence of the Kalman filter estimates to Wiener filter estimates in the absence of noise in the state [39].

The good performance of the point process adaptive filter algorithm in estimating the true parameter values of the model was also supported by KS plot assessment, measuring the agreement between the model with the dynamic parameter estimates and the simulated heartbeat series. The KS plot of the estimated transformed intervals was within the 95% confidence intervals of Fig. 1(e). Moreover, consistent with the transformed intervals being independent as predicted by the time-rescaling theorem, the autocorrelation function of the transformed intervals was indistinguishable from zero up to lag 60, or approximately 50 s [Fig. 1(e)]. These findings suggested good agreement between the simulated HDIG heartbeat interval series and the HDIG model with its parameters estimated dynamically by the point process adaptive filter. It, therefore, shows the ability of the algorithm to estimate nontime-varying parameters.

B. Analysis of Simulated Heartbeat Series With Time-Varying Parameters

To test the ability of our algorithm to track the changes in the HDIG model parameters, we simulated 20 1600-s realizations of an AR(2) HDIG model in which each of four model parameters underwent a different change at different points in time [Fig. 2(a) and (b), gray lines]. The parameter θ_0 was constant at 834 ms from 0 to 500 s, decreased linearly from 834 ms to 778 ms between times 500 and 745 s and remained constant at 778 ms for the balance of the simulation [Fig. 2(a.1) and (b.1), gray line]. The variance σ_s^2 was constant at 1500 ms^2 from 0 to 625 s, increased instantaneously to 3000 ms^2 at time 625 s, remained constant at 3000 ms^2 from 625 s to 1020 s, at which point it returned instantaneously to 1500 ms^2 where it remained for the balance of the simulation [Fig. 2(a.2) and (b.2), gray line]. The parameter θ_1 was constant at -0.1 from 0 to 400 s, decreased linearly to -0.2 from 400 to 500 s and remained constant at -0.2 for the balance of the simulation [Fig. 2(a.3) and (b.3), gray line]. The parameter θ_2 was constant at -0.25 from 0 to 1000 s, increased linearly to -0.15 from 1000 s to 1100 s and remained at -0.15 for the balance of the simulation [Fig. 2(a.4) and (b.4), thin gray line].

By doing a preliminary fit of the heartbeat probability model using local maximum likelihood we found a range of values for the diagonal elements of W_ε between 10^{-9} and 10^{-1}. Using this range we chose the state covariance matrix W_ε to be the diagonal matrix with values of 3×10^{-1} for θ_0, 4×10^{-2} for σ_s^2, and 4×10^{-7} for the autoregressive parameters. This choice of W_ε gave a reliable performance of the algorithm. We compared the performance of our point process adaptive filter algorithm with that of the widely-used recursive least-squares (RLS) algorithm computing time-varying indices of HRV in the analysis of the 20 realizations. We constructed the RLS algorithm using an AR(2) model with a forgetting factor of 0.98 [6]. We chose the value of 0.98 for the forgetting factor because it balanced well the bias-variance tradeoff. The RLS algorithm updates the parameters only when a beat occurs and provides no estimate of θ_0, because this algorithm requires that the $R{-}R$ series first be detrended with a high-pass filter [6]. Fig. 2(a.1), (a.2), and (a.4) shows that point process adaptive filter estimates (bold curves) tracked well the time courses of θ_0, σ_s^2 and θ_2, respectively, in that single realization. For this particular realization, the algorithm also tracked the time course of θ_1 but with more variation about the true parameter value [Fig. 2(a.3), bold curve]. The RLS algorithm estimates [Fig. 2(a.2), (a.3), and (2a.4), thin curves] agreed less closely with the true time course of the parameters σ_s^2, θ_1 and θ_2 than the point process filter algorithm. The RLS estimate shows less variability in σ_s^2 and more variability in the autoregressive parameters than the corresponding HDIG estimates.

Fig. 2(b) shows the average trajectory estimates for each parameter computed from the 20 realizations for the point process adaptive filter (bold curves) and the RLS filter (thin curves) algorithms. The point process adaptive filter algorithm estimates are in closer agreement with the true time course of the parameter trajectories than the RLS estimates. In particular, the averaged trajectories [Fig. 2(b)] show the slower tracking of the

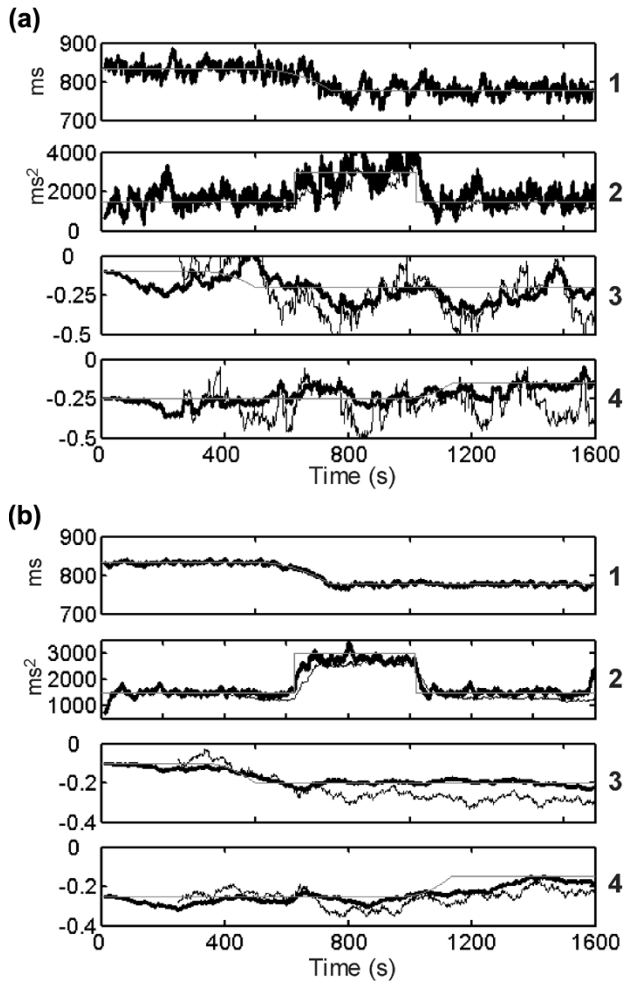

Fig. 2. (a) Instantaneous time varying estimates of 1—the mean $R{-}R$, 2— $R{-}R$ variance and 3 and 4—the autoregressive coefficients obtained by applying our algorithm (bold lines) and an adaptive RLS algorithm with a forgetting factor of 0.98 (thin lines) to an AR(2) simulated beat series where the four parameters undergo sudden changes at different moments in time. (b) Instantaneous time varying estimates averaged over 20 realizations.

$R{-}R$ variance by the RLS algorithm. This is most evident in Fig. 2(b.2) after the step change at 625 s, where the averaged RLS estimate shows a slower exponential approach to the new true value than the approach of the HDIG estimate.

The KS plots of the transformed times for each of the 20 estimated heartbeat series from the point process adaptive filter algorithm were all within the 95% confidence bounds and the autocorrelations functions of the transformed times were all indistinguishable from zero (not shown). This suggests that in each realization, the point process adaptive filter algorithm computed an accurate estimate of the stochastic structure in the simulated heartbeat series.

C. Analysis of Heartbeat Series From a Tilt Table Study

To illustrate the application of our point process adaptive filter algorithm to actual data, we analyzed the 3000 s heartbeat series from a male subject performing a tilt table study [Fig. 3(a)]. The study began with the subject lying supine for 11 min, after which, the subject underwent three types of up-down tilt pairs. The tilt pairs were: rapid up (down) tilt in which, at time 664

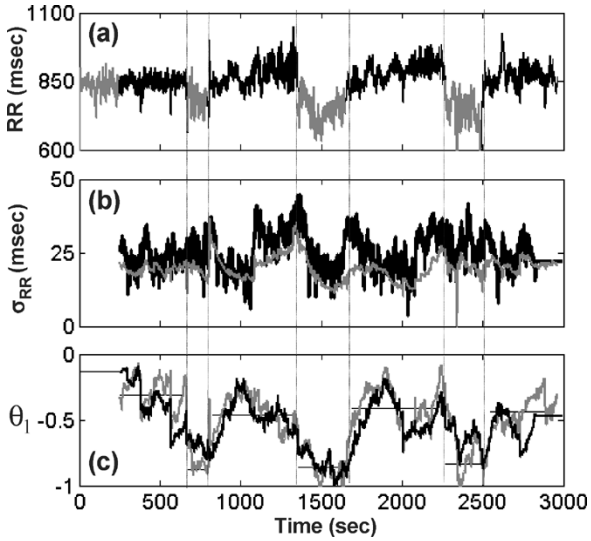

Fig. 3. (a) $R-R$ interval data from one continuous recording of the tilt protocol. The first 200 s segment (gray) is used for computing initial parameters' estimates, the black segments refer to epochs in which the subject is in the supine position, whereas the gray segments refer, in order, to the rapid tilt up-down, slow tilt up-down, and stand up-down procedures. (b) $R-R$ standard deviation and (c) first autoregressive coefficient estimated by our model (black curves) and by the RLS model (gray curves). The black constant lines in (c) refer to values of the respective autoregressive coefficient estimated by a stationary AR(8) yule-walker algorithm applied to each of the gray and black segments plotted in (a).

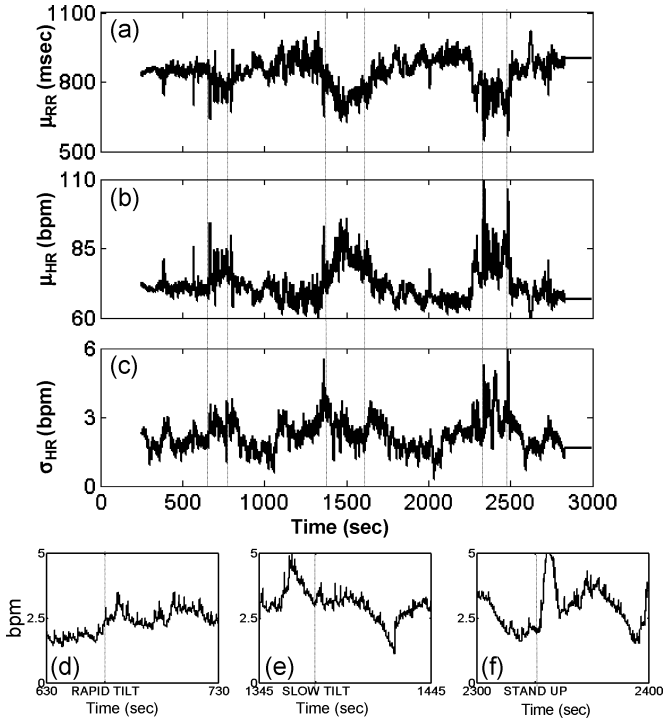

Fig. 4. Instantaneous time varying estimates of the (a) mean $R-R$, (b) heart rate, (c) heart rate standard deviation as defined in (14)–(17). Dotted lines delimit the rapid tilt up-down, slow tilt up-down, and stand up-down procedures. (d)–(f) Zoom of the heart rate variance estimates in (c) during the three gravitational transients. (d) Rapid tilt. (e) Slow tilt. (f) Stand up.

(792) s, the tilt table moved from horizontal (vertical) to vertical (horizontal) in less than 3 s; slow up (down) tilt in which the tilt table, starting at time 1379 (1622) s, moved from horizontal (vertical) to vertical (horizontal) in approximately 1 min; and stand-up (supine) in which the subject stood up immediately supporting his or her own weight at time 2331 s and, at time 2479 s, lied supine immediately from having been standing supporting his own weight [40], [41].

Following a preliminary partial autocorrelation analysis of the $R-R$ interval series, we implemented the point process adaptive filter algorithm assuming an AR(8) HDIG model to analyze these data. The initial parameter values were computed by local maximum likelihood analysis using the first 200 s [Fig. 4(a), gray segment]. We chose the state covariance matrix W_ε to be the diagonal matrix with values of 3×10^{-2} for θ_0, 2×10^{-2} for σ_s^2, and 8×10^{-7} for the autoregressive parameters by applying the same preliminary local maximum likelihood analysis used in the previous section. In Fig. 4(a), the black segments are epochs in which the subject was supine, whereas the gray segments are, in order, the rapid up-down tilt, the slow up-down tilt, and stand up-down.

Our $R-R$ standard deviation estimates [Fig. 3(b), black curve] show rapid changes, especially prominent after each up and down postural change. These fast fluctuations are not noticeable in the RLS beat-to-beat estimate [Fig. 3(b), gray curve]. On the other hand, the HDIG estimate of θ_1 [Fig. 3(c), black curve] shows fluctuations similar to those of the RLS estimate [Fig. 3(c), gray curve]. For a more complete comparison, in each colored segment, we treated the data as stationary and computed the Yule–Walker estimates of the autoregression parameter [Fig. 3(c), black horizontal lines]. The local Yule–Walker estimates are consistent with both time-varying estimates. However, these static interval estimates obscure the dynamic behavior of the parameter trajectory.

A compelling feature of our analysis is that it provided time-varying estimates of mean $R-R$ [Fig. 4(a)], heart rate [Fig. 4(b)], $R-R$ standard deviation [Fig. 3(b)], and heart rate standard deviation [Fig. 4(c)] computed using (14)–(17). The increase in the heart rate standard deviation immediately after the rapid tilt [Fig. 4(d)], the constant level the heart rate standard deviation after the slow tilt [Fig. 4(e)], and the much sharper increase immediately after standing up [Fig. 4(f)] suggest new patterns of fast dynamics which may be useful to distinguish physiological differences in these states. Most importantly, the $R-R$ and heart rate standard deviations show that time-varying estimates of mean $R-R$ and heart rate alone do not capture all the dynamic features of heartbeat interval.

Although we used the AR(8) HDIG in conducting the analysis, we tried AR HDIG models of order 2 and 4 as well. The goodness-of-fit analysis gave essentially identical KS plots for the three models [Fig. 5(a)]. Except for a small interval between 0.75 and 0.85, the KS plot for all these model fits lies entirely within the 95% confidence bounds [Fig. 5(a)]. In other words, the KS plot alone did not help to distinguish the models. Therefore, because under the time-rescaling theorem the transformed times should be independent and hence, uncorrelated, we further assessed goodness-of-fit by comparing the autocorrelation function of the transformed times for the HDIG model of order 2 [Fig. 5(b)], 4 [Fig. 5(c)], and 8 [Fig. 5(d)]. Both the AR(2) and the AR(4) have several autocorrelation lag estimates that fell outside the 95% confidence bounds. All are smaller than 0.14. This suggests that there were still some correlations in the

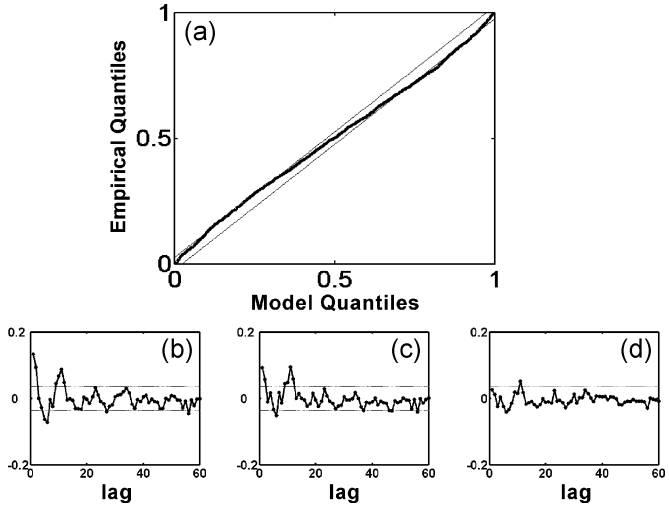

Fig. 5. (a) KS plot of the time-rescaled quantiles derived from the tilt protocol AR(8) parameters' estimates. (b)–(d) Autocorrelation function the transformed times estimated for the first 60 lags by analysis of one continuous recording of the tilt protocol using (b) AR(2), (c) AR(4), and (d) AR(8) models. The horizontal lines are the approximate 95% confidence intervals.

transformed times of these models. In contrast, for the AR(8) model, the largest autocorrelation coefficient is 0.05 at lag 11 [Fig. 5(d)] suggesting that its transformed times are more nearly independent. In summary, the goodness-of-fit analysis suggests that the AR(8) HDIG model with time-varying parameters describes well the stochastic structure in this subject's heartbeat series.

D. Analysis of Heartbeat Series from Healthy Subjects and Subjects With Congestive Heart Failure

To illustrate the use of our HRV indices to distinguish physiological and pathological conditions, we analyzed heartbeat recordings from 15 healthy subjects and 12 subjects with severe congestive heart failure (CHF) taken from the PhysioNet database [42]. A 50 min segment beginning at 12:00 am for each subject was analyzed. To each subject's heartbeat series we fit the HDIG AR(8) model using the W_ε as chosen in the previous example and computed instantaneous estimates of mean R–R, heart rate, R–R standard deviation, and heart rate standard deviation. We averaged the instantaneous estimates to compute a single summary for each index for each subject. We assessed the difference in the means of the four indices for each group using a two-sample t-test and, because there were only 15 and 12 subjects per group, a Wilcoxon rank sum test (Table I).

Each of the four indices was significantly different between the CHF subjects compared with the healthy subjects. In particular, the average of σ_{RR} and the average of σ_{HR} were significantly smaller for the CHF subjects demonstrating, as has been previously reported, that the CHF subjects had less variability [1] (Table I). For comparison with established measures of HRV, we performed a similar analysis using the RLS algorithm with its parameter settings as chosen in the previous example and the standard measure of HRV computed from the standard deviation of the R–R intervals index (SDNN index) [1]. A similar, significant decrease in variability of the CHF subjects relative to the healthy subjects was also demonstrated with these two indices (Table I). These results demonstrate that summary measures computed from our instantaneous indices of heartbeat dynamics can be used to distinguish healthy from pathological conditions and that these summaries give results consistent with established measures.

TABLE I
COMPARISON BETWEEN HEALTHY SUBJECTS AND SUBJECTS WITH CONGESTIVE HEART FAILURE OF THE HDIG INDICES, ALONG WITH THE R–R STANDARD DEVIATION COMPUTED BY THE RLS ALGORITHM AND BY A STANDARD METHOD (SDNN INDEX)

	Healthy	CHF	p (t-test)	p (Rank Sum)
HDIG	(mean ± sd)	(mean ± sd)		
μ_{RR}, ms	893 ± 128	704 ± 137	6.4×10^{-4}	1.9×10^{-3}
μ_{HR}, bpm	69.1 ± 9.7	88.3 ± 16.8	1.3×10^{-3}	1.9×10^{-3}
σ_{RR}, ms	33.2 ± 15.5	12.0 ± 3.1	5.8×10^{-5}	1.9×10^{-5}
σ_{HR}, bpm	2.5 ± 0.7	1.5 ± 0.5	1.9×10^{-4}	1.4×10^{-4}
RLS				
σ_{RR}, ms	32.2 ± 18.6	9.4 ± 3.2	1.6×10^{-4}	3.0×10^{-5}
TASK FORCE				
SDNN index, ms	63.6 ± 23.9	18.4 ± 10.6	1.1×10^{-6}	2.4×10^{-5}

IV. DISCUSSION

We developed a point process adaptive filter algorithm to study heartbeat dynamics. The algorithm is based on the inverse Gaussian probability model because this model can be derived as a stochastic version of the widely-applied deterministic integrate-and-fire models used to simulate heartbeats. We used an autoregressive model to define the mean of the inverse Gaussian and to represent the dependence of the R–R interval length on the recent state of the autonomic inputs to the SA node. The point process adaptive filter was used to estimate the time-varying nature of the inputs to the SA node. Because the point process heartbeat model was defined in continuous time, the algorithm computed estimates of mean R–R, R–R standard deviation, mean heart rate and heart rate standard deviation that can be updated at any desired temporal resolution.

We obviated interpolation because our heart rate probability model (4) gave a precise probabilistic prescription for how to convert the point process R-wave events into heart rate and the other HRV indices. Our approach makes use of the well-documented fact that use of continuous time models and state estimation, rather than simple interpolation, offers a more principled approach to estimating an unobserved quantity at times where no observation is recorded [38]. Because the probability model is defined in continuous time, we can compute the same indices under stationary conditions using maximum likelihood [25] and under nonstationary conditions using the point process adaptive filter algorithm developed here. Furthermore, because the conditional intensity function gives a canonical characterization of a point process, we used the estimated conditional intensity function to construct goodness-of-fit tests by the time-rescaling theorem. Our goodness-of-fit tests allowed us to compare different point process heartbeat models to help select the order of history dependence and to assess how well the models describe the data.

The heartbeat model in (1) differs from a standard stationary autoregression model. A stationary autoregressive model of order p is typically a model of a continuous-valued Gaussian process with constant coefficients and a white noise variance sampled at discrete, equally-spaced time points [43]. In contrast, a point process is a discrete-valued process that occurs in continuous time [36], [37]. The autoregression for our point process model in (1) is constructed by assuming that the R-wave events obey an inverse Gaussian model and that the mean of the current R–R interval can be expressed as a linear function of the p previous R–R intervals. Because our autoregression is on the R–R intervals, the time points at which these coefficients are computed are not evenly spaced. Furthermore, by construction our model is nonstationary with both time-varying autoregressive coefficients and process variance. The RLS method also offers a method of computing time-varying estimates for an autoregressive model. However, it treats the R–R intervals as if they are evenly-spaced, and models the R–R intervals as Gaussian observations instead of as a point process. Moreover, unlike the adaptive filter algorithm, which can compute updates at any desired temporal resolution, the RLS algorithm only computes updates when a heartbeat is observed.

The simulation studies showed that our point process adaptive filter algorithm estimated well the heartbeat dynamics under stationary conditions and in the presence of either gradual or abrupt changes in the temporal structure of the heartbeats. The performance of our physiologically-motivated algorithm suggests a way of improving upon the established RLS algorithm. The HRV indices we computed in the tilt table study suggest a set of dynamic signatures that may be used to characterize the dynamic range of the cardiovascular responses under different physiological conditions. The differences in our HRV indices between the normal subjects and congestive heart failure subjects illustrate how these metrics may be used to distinguish normal and pathological conditions.

Several extensions of the current framework are possible. First, gaining more experience in the choice of W_ε will help broaden application of the methods. Second, it will be valuable to study our new time domain and frequency domain measures of heartbeat dynamics in other protocols to establish their physiological relevance. Third, the new algorithm may be used to monitor heartbeat dynamics in clinical setting such as the intensive care unit, the operating room and during labor and delivery. Fourth, the predictions made by the point process adaptive filter algorithm may be used to identify and replace ectopic beats. Finally, we will investigate inclusion of these methods into state-space [44] multivariate models of cardiovascular control and autonomic regulation [4], [45].

ACKNOWLEDGMENT

The authors are grateful to R. G. Mark and T. Heldt, Harvard-Massachusetts Institute of Technology Division of Health Sciences and Technology, for kindly providing the tilt-table data analyzed in this paper. This work was initiated while E.N. Brown was on sabbatical at the Laboratory for Decision Systems in the Department of Electrical Engineering and Computer Science at Massachusetts Institute of Technology.

REFERENCES

[1] M. Malik and A. Camm, and Members of the Task Force, "Heart rate variability: standards of measurement, physiological interpretation, and clinical use," *Circulation*, vol. 93, pp. 1043–1065, 1996.

[2] S. Akselrod, D. Gordon, F. A. Ubel, D. C. Shannon, A. C. Berger, and R. J. Cohen, "Power spectrum analysis of heart rate fluctuation: a quantitative probe of beat-to-beat cardiovascular control," *Science*, vol. 213, pp. 220–222, 1981.

[3] M. Pagani, G. Malfatto, S. Pierini, R. Casati, A. Masu, M. Poli, S. Guzzetti, F. Lombardi, S. Cerutti, and A. Malliani, "Spectral analysis of heart rate variability in the assessment of autonomic diabetic neuropathy," *J. Auton. Nerv. Syst.*, vol. 23, pp. 143–153, 1988.

[4] R. Barbieri, A. M. Bianchi, J. K. Triedman, L. T. Mainardi, S. Cerutti, and J. P. Saul, "Model dependency of multivariate autoregressive spectral analysis: quantifying cardiovascular control using bivariate and trivariate models," *IEEE Eng. Med. Biol. Mag.*, vol. 16, no. 5, pp. 74–85, Sep.-Oct. 1997.

[5] R. Barbieri, R. A. Waldmann, V. Di Virgilio, J. K. Triedman, A. M. Bianchi, S. Cerutti, and J. P. Saul, "Continuous quantification of baroreflex and respiratory control of heart rate by use of bivariate autoregressive techniques," *Ann. Noninvasive Electrocardiol.*, vol. 1, pp. 264–277, 1996.

[6] A. M. Bianchi, L. Mainardi, E. Petrucci, M. G. Signorini, M. Mainardi, and S. Cerutti, "Time-variant power spectrum analysis for the detection of transient episodes in HRV signal," *IEEE Trans. Biomed. Eng.*, vol. 40, no. 2, pp. 136–144, Feb. 1993.

[7] S. Cerutti, G. Baselli, A. M. Bianchi, L. T. Mainardi, M. G. Signorini, and A. Malliani, "Cardiovascular variability signals: from signal processing to modeling complex physiological interactions," *Automedica*, vol. 16, pp. 45–69, 1994.

[8] J. P. Saul, R. D. Berger, P. Albrecht, S. P. Stein, M. H. Chen, and R. J. Cohen, "Transfer function analysis of the circulation: unique insights into cardiovascular regulation," *Am. J. Physiol. Heart Circ. Physiol.*, vol. 261, pp. H1231–H1245, 1991.

[9] P. C. Ivanov, L. A. Amaral, A. L. Goldberger, S. Havlin, M. G. Rosenblum, Z. R. Struzik, and H. E. Stanley, "Multifractality in human heartbeat dynamics," *Nature*, vol. 399, pp. 461–465, 1999.

[10] P. C. Ivanov, M. G. Rosenblum, C. K. Peng, J. Mietus, S. Havlin, H. E. Stanley, and A. L. Goldberger, "Scaling behavior of heartbeat intervals obtained by wavelet-based time-series analysis," *Nature*, vol. 383, pp. 323–327, 1996.

[11] C. S. Poon and C. K. Merrill, "Decrease of cardiac chaos in congestive heart failure," *Nature*, vol. 389, pp. 492–495, 1997.

[12] G. Sugihara, W. Allan, D. Sobel, and K. D. Allan, "Nonlinear control of heart rate variability in human infants," *Proc. Nat. Acad. Sci.*, vol. 93, pp. 2608–2613, 1996.

[13] S. M. Pincus and A. L. Goldberger, "Physiological time-series analysis: what does regularity quantify?," *Am. J. Physiol.*, vol. 266, pp. H1643–H1656, 1994.

[14] J. Hayano, J. A. Taylor, A. Yamada, S. Mukai, R. Hori, T. Asakawa, K. Yokoyama, Y. Watanabe, K. Takata, and T. Fujinami, "Continuous assessment of hemodynamic control by complex demodulation of cardiovascular variability," *Am. J. Physiol. Heart. Circ. Physiol.*, vol. 264, pp. H1229–H1238, 1993.

[15] S. Joho, H. Asanoi, H. A. Remah, A. Igawa, T. Kameyama, T. Nozawa, K. Umeno, and H. Inoue, "Time-varying spectral analysis of heart rate and left ventricular pressure variability during balloon coronary occlusion in humans: a sympathoexcitatory response to myocardial ischemia," *J. Am. Coll. Cardiol.*, vol. 34, pp. 1924–1931, 1999.

[16] Y. Kimura, K. Okamura, T. Watanabe, N. Yaegashi, S. Uehara, and A. Yajima, "Time-frequency analysis of fetal heartbeat fluctuation using wavelet transform," *Am. J. Physiol. Heart Circ. Physiol.*, vol. 275, pp. H1993–H1999, 1998.

[17] V. Novak, P. Novak, J. de Champlain, A. R. Le Blanc, R. Martin, and R. Nadeau, "Influence of respiration on heart rate and blood pressure fluctuations," *J. Appl. Physiol.*, vol. 74, pp. 617–626, 1993.

[18] E. Toledo, O. Gurevitz, H. Hod, M. Eldar, and S. Akselrod, "Wavelet analysis of instantaneous heart rate: a study of autonomic control during thrombolysis," *Am. J. Physiol. Regul. Integr. Comp. Physiol.*, vol. 284, pp. R1079–R1091, 2003.

[19] V. Pichot, J. M. Gaspoz, S. Molliex, A. Antoniadis, T. Busso, F. Roche, F. Costes, L. Quintin, J. R. Lacour, and J. C. Barthelemy, "Wavelet transform to quantify heart rate variability and to assess its instantaneous changes," *J. Appl. Physiol.*, vol. 86, pp. 1081–1091, 1999.
[20] Y. Yamamoto and R. L. Hughson, "Coarse graining spectral analysis: new method for studying heart rate variability," *J Appl Physiol*, vol. 71, pp. 1143–1150, 1991.
[21] L. T. Mainardi, A. M. Bianchi, G. Baselli, and S. Cerutti, "Pole-tracking algorithms for the extraction of time-variant heart rate variability spectral parameters," *IEEE Trans. Biomed. Eng.*, vol. 42, no. 3, pp. 250–259, Mar. 1995.
[22] E. N. Brown, D. A. Nguyen, L. M. Frank, M. A. Wilson, and V. Solo, "An analysis of neural receptive field plasticity by point process adaptive filtering," *Proc. Nat. Acad. Sci.*, vol. 98, pp. 12 261–12 266, 2001.
[23] R. Barbieri, L. M. Frank, D. P. Nguyen, M. C. Quirk, V. Solo, and E. N. Brown, "Dynamic analyses of information encoding in neural ensembles," *Neural Computation*, vol. 16, pp. 277–307, 2004.
[24] U. T. Eden, L. M. Frank, R. Barbieri, V. Solo, M. A. Wilson, and E. N. Brown, "Dynamic analysis of neural encoding by point process adaptive filtering," *Neural Computation*, vol. 16, pp. 971–998, 2004.
[25] R. Barbieri, E. C. Matten, A. A. Alabi, and E. N. Brown, "A point process model of human heart rate intervals: new definitions of heart rate and heart rate variability," *Am. J. Physiol. Heart. Circ. Physiol.*, vol. 288, pp. H424–4H35, 2005.
[26] E. N. Brown, R. Barbieri, V. Ventura, R. E. Kass, and L. M. Frank, "The time-rescaling theorem and its application to neural spike train data analysis," *Neural Computation*, vol. 14, pp. 325–346, 2002.
[27] A. C. Guyton, *Textbook of Medical Physiology*, 8th ed, PA: Harcourt Brace, 1991.
[28] R. W. De Boer, J. M. Karemaker, and J. Strackee, "Spectrum of a series of point event, generated by the integral pulse frequency modulation model," *Med. Biol. Eng. Comput.*, vol. 23, pp. 138–142, 1985.
[29] R. D. Berger, S. Akselrod, D. Gordon, and R. J. Cohen, "An efficient algorithm for spectral analysis of heart rate variability," *IEEE Trans. Biomed. Eng.*, vol. BME-33, pp. 900–904, 1986.
[30] H. C. Tuckwell, *Introduction to Theoretical Neurobiology*. New York: Cambridge Univ. Press, 1988, vol. 2, Nonlinear and Stochastic Theories.
[31] G. B. Stanley, K. Poolla, and R. A. Siegel, "Threshold modeling of autonomic control of heart rate variability," *IEEE Trans. Biomed. Eng.*, vol. 47, no. 9, pp. 1147–1153, Sep. 2000.
[32] R. J. L. Leor-Librach, S. Eliash, E. Kaplinsky, and B. Bobrovsky, "Very low-frequency heart rate variability wave amplitude and sympathetic stimulation-characterization and modeling," *IEEE Trans. Biomed. Eng.*, vol. 50, no. 7, pp. 797–803, Jul. 2003.
[33] K. L. Fernando, V. J. Mathews, M. W. Varner, and E. B. Clark, "Robust estimation of fetal heart rate variability using Doppler ultrasound,," *IEEE Trans. Biomed. Eng.*, vol. 50, no. 8, pp. 950–957, Aug. 2003.
[34] S. R. Seydnejad and R. Kitney, "Real-time heart rate variability extraction using the Kaiser window," *IEEE Trans. Biomed. Eng.*, vol. 44, no. 10, pp. 990–1005, Oct. 1997.
[35] J. Mateo and P. Laguna, "Analysis of heart rate variability in the presence of ectopic beats using the heart timing signal," *IEEE Trans. Biomed. Eng.*, vol. 50, no. 3, pp. 334–343, Mar. 2003.
[36] R. S. Chhikara and J. L. Folks, *The Inverse Gaussian Distribution: Theory, Methodology, and Applications*. New York: Marcel Dekker, 1989.
[37] E. N. Brown, R. Barbieri, U. T. Eden, and L. M. Frank, "Likelihood methods for neural data analysis," in *Computational Neuroscience: A Comprehensive Approach*, J. Feng, Ed. London, U.K.: Chapman & Hall, 2003, ch. 9, pp. 253–286.
[38] G. Kitagawa and W. Gersh, *Smoothness Priors Analysis of Time Series*. New York: Springer, 1996.
[39] J. M. Mendel, *Lessons in Estimation Theory for Signal Processing, Communications, and Control*. Englewood Cliffs, NJ: Prentice-Hall, 1995.
[40] T. Heldt, E. B. Shim, R. D. Kamm, and R. G. Mark, "Computational modeling of cardiovascular response to orthostatic stress," *J. Appl. Physiol.*, vol. 92, pp. 1239–1254, 2002.
[41] T. Heldt, M. B. Oefinger, M. Hoshiyama, and R. G. Mark, "Circulatory response to passive and active changes in posture," in *Proc. Computers in Cardiology*, 2003, pp. 263–266.
[42] A. L. Goldberger, L. A. N. Amaral, L. Glass, J. M. Hausdorff, P. C. Ivanov,, R. G. Mark, J. E. Mietus, G. B. Moody, C. K. Peng, and H. E. Stanley, "PhysioBank, PhysioToolkit, and PhysioNet: components of a new research resource for complex physiologic signals," *Circulation*, vol. 101, no. 23, pp. e215–e220, Jun. 2000.
[43] G. E. P. Box, G. M. Jenkins, and G. C. Reinsel, *Time Series Analysis, Forecasting and Control*, 3rd ed. Englewood Cliffs, NJ: Prentice-Hall, 1994.
[44] A. C. Smith and E. N. Brown, "Estimating a state-space model from point process observations," *Neural Computation*, vol. 15, pp. 965–991, 2003.
[45] L. T. Mainardi, A. M. Bianchi, R. Furlan, S. Piazza, R. Barbieri, V. Di Virgilio, A. Malliani, and S. Cerutti, "Multivariate time-variant identification of cardiovascular variability signals: a beat-to-beat spectral parameter estimation in vasovagal syncope," *IEEE Trans. Biomed. Eng.*, vol. 44, no. 10, pp. 978–989, Oct. 1997.

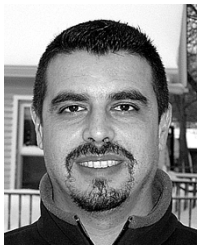

Riccardo Barbieri (M'00) was born in Rome, Italy, in 1967. He received the M.S. degree in electrical engineering from the University of Rome "La Sapienza," Rome, Italy, in 1992, and the Ph.D. degree in biomedical engineering from Boston University, Boston, MA, in 1997.

He is currently Instructor in Anaesthesia at Harvard Medical School and Research Associate at Massachusetts General Hospital. His main research interests are in the development of signal processing algorithms for analysis of biological systems. He is currently focusing his studies on computational modeling of neural information encoding, and on application of multivariate and statistical models to characterize heart rate and heart rate variability as related to cardiovascular control dynamics.

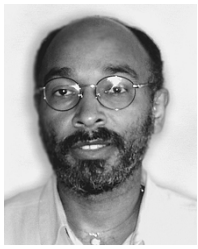

Emery N. Brown (M'01) received the B.A. degree from Harvard College, Cambridge, MA, the M.D. degree from Harvard Medical School, Boston, MA, and the A.M. and Ph.D. degrees in statistics from Harvard University, Cambridge, MA.

He is presently Professor of Computational Neuroscience and Health Sciences and Technology in the Department of Brain and Cognitive Sciences and the MIT-Division of Health Sciences and Technology at Massachusetts Instiute of Technology, Associate Professor of Anaesthesia at Harvard Medical School, and Director of the Neuroscience Statistics Research Laboratory and an Anesthesiologist in the Department of Anesthesia and Critical Care at Massachusetts General Hospital. His research interests are in the development of signal processing algorithms and point process methods for the analysis of neural systems.

Dr. Brown is a member of the Association of University of Anesthesiologists and the Committee of Applied and Theoretical Statistics of the National Academies.